Georgia Institute of Technology
STATE ENGINEERING EXPERIMENT STATION
Atlanta, Georgia

FINAL REPORT

PROJECT NO. 194

THE NORMAL COMPONENT OF THE INDUCED VELOCITY IN THE VICINITY OF A LIFTING ROTOR AND SOME EXAMPLES OF ITS APPLICATION

By

Walter Castles, Jr. and Jacob Henri De Leeuw

- o - o - o - o -

CONTRACT NO. NAw - 6124

NATIONAL ADVISORY COMMITTEE FOR AERONAUTICS

- o - o - o - o -

APRIL 1952

Georgia Institute of Technology
STATE ENGINEERING EXPERIMENT STATION
Atlanta, Georgia

FINAL REPORT

PROJECT NO. 194

THE NORMAL COMPONENT OF THE INDUCED VELOCITY IN THE VICINITY OF A LIFTING ROTOR AND SOME EXAMPLES OF ITS APPLICATION

By

Walter Castles, Jr. and Jacob Henri De Leeuw

- o - o - o - o -

CONTRACT NO. NAw - 6124

NATIONAL ADVISORY COMMITTEE FOR AERONAUTICS

- o - o - o - o -

APRIL 1952

TABLE OF CONTENTS

	Page
SUMMARY	1
INTRODUCTION	1
NOTATION	3
ANALYSIS	6
A. The Velocity Induced by a Vortex Ring	6
B. The Normal Component of the Induced Velocity in the Vicinity of a Lifting Rotor	8
RESULTS	11
APPLICATION OF RESULTS	12
A. The Determination of the Mean Value of the Normal Component of the Induced Velocity Over the Front and Back Rotors of a Tandem-Rotor Helicopter	12
B. The Determination of the Longitudinal Variation of the Normal Component of the Induced Velocity over the Front and Back Rotors of a Tandem-Rotor Helicopter	14
C. The Determination of the Induced Flow Angle at a Horizontal Tailplane	15
CONCLUDING DISCUSSION	16
REFERENCES	19
APPENDIX	20

LIST OF TABLES

		Page
I.	NONDIMENSIONAL VALUES OF THE NORMAL COMPONENT OF THE INDUCED VELOCITY IN THE VICINITY OF A VORTEX RING.	21
II.	NONDIMENSIONAL VALUES OF THE NORMAL COMPONENT OF THE INDUCED VELOCITY IN THE LONGITUDINAL PLANE OF SYMMETRY OF A LIFTING ROTOR FOR 90°	29
III.	NONDIMENSIONAL VALUES OF THE NORMAL COMPONENT OF THE INDUCED VELOCITY ON THE LATERAL AXIS OF A LIFTING ROTOR.	36

LIST OF FIGURES

1.	COORDINATES FOR VORTEX RING AND TABLE I.	37
2.	NONDIMENSIONAL ROTOR COORDINATES	38
3.	GEOMETRY OF WAKE	39
4.	ISO-INDUCED VELOCITY LINES FOR $\chi = 0° = \tan^{-1} 0$.	40
5.	ISO-INDUCED VELOCITY LINES FOR $\chi = 14.0° = \tan^{-1} 1/4$ . . .	41
6.	ISO-INDUCED VELOCITY LINES FOR $\chi = 26.5° = \tan^{-1} 1/2$ . . .	42
7.	ISO-INDUCED VELOCITY LINES FOR $\chi = 45.0° = \tan^{-1} 1$	43
8.	ISO-INDUCED VELOCITY LINES FOR $\chi = 63.4° = \tan^{-1} 2$	44
9.	ISO-INDUCED VELOCITY LINES FOR $\chi = 76.0° = \tan^{-1} 4$	45
10.	ISO-INDUCED VELOCITY LINES FOR $\chi = 90.0° = \tan^{-1}$	46
11.	ISO-INDUCED VELOCITY LINES FOR $\chi = 104.0° = \tan^{-1} -4$ . . .	47
12.	ISO-INDUCED VELOCITY LINES FOR $\chi = 116.6° = \tan^{-1} -2$ . . .	48
13.	INDUCED VELOCITY DISTRIBUTIONS ALONG THE LONGITUDINAL AXIS.	49
14.	INDUCED VELOCITY DISTRIBUTIONS ALONG THE LATERAL AXIS	50

This Report Contains 50 Pages

THE NORMAL COMPONENT OF THE INDUCED VELOCITY IN THE VICINITY OF A LIFTING ROTOR AND SOME EXAMPLES OF ITS APPLICATION

SUMMARY

This paper presents a practical method for computing the approximate values of the normal component of the induced velocity at points in the flow field of a lifting rotor. Tables and graphs of the relative magnitudes of the normal component of the induced velocity are given for selected points in the longitudinal plane of symmetry of the rotor and on the lateral rotor axis. These are presented in the appendix.

A method is also presented for utilizing the tables and graphs to determine the interference induced velocities arising from the second rotor of a tandem or side-by-side rotor helicopter and the induced flow angle at a horizontal tailplane.

INTRODUCTION

This work, sponsored by the National Advisory Committee for Aeronautics and the Georgia Institute of Technology State Engineering Experiment Station, was undertaken in an attempt to obtain a better understanding of the induced flow in the vicinity of a lifting rotor.

Previous investigations, such as those of references 1 and 2, demonstrated that the solution of the integral for the normal component of the induced velocity at the center of the rotor could be obtained in an elementary form provided certain approximations were made as to the distribution of vorticity in the wake. However, the value of the integral for the induced velocity component at an arbitrary point in

the rotor flow field cannot, in general, be expressed in terms of elementary functions. Its numerical evaluation for a specific case presents considerable difficulty.

The junior author, in reference 3, investigated the feasibility of calculating the induced velocity at arbitrary points in the vicinity of the rotor by an alternative method which consisted of (1) numerically integrating the increments induced by the vortex ring wake elements within a given distance of the point and (2) summing up the effect of the remainder of the wake by an approximate integral. This approach is quite general in that it can be applied to any wake which can be approximated by an assembly of vortex rings. It was found that the method afforded satisfactory accuracy with the expenditure of a reasonable amount of effort, since the values of the normal induced velocity component for the isolated rings may be precomputed and tabulated for repeated use.

The scope of the present paper is limited principally to a consideration of the values of the normal component of the induced velocity at points in the longitudinal plane of symmetry and within the region likely to be occupied by the second rotor of a tandem-rotor helicopter. In addition, the values of the normal component of the induced velocity were calculated for points on the lateral axis of the tip-path plane over the distance of interest for the case of a helicopter with laterally disposed rotors.

In view of the present lack of experimental evidence as to the actual wake distribution of vorticity, the calculations for the present paper were based on the same assumptions for the wake shape as those

found in references 1 and 2. These assumptions were that the wake vortex distribution consists of a straight eliptic cylinder formed by a uniform, continuous distribution of vortex rings of infinitesimal strength, lying in planes parallel to the tip-path plane and extending downstream to infinity.

NOTATION

a_1 coefficient of the cosine term of the Fourier series for the blade flapping angle $\beta = a_o - a_1 \cos\psi - b_1 \sin \quad - \ . \ . \ .$

b_1 coefficient of the sine component of the flapping angle

C_T thrust coefficient $\frac{T}{\rho\pi\Omega^2R^4}$

d_1 nondimensional shortest distance from a point P to a vortex ring (figure 1) $\sqrt{z^2 + (x-1)^2}$

d_2 nondimensional largest distance from a point P to a vortex ring (figure 1) $\sqrt{z^2 + (x+1)^2}$

D_f drag of the fuselage

$E(\tau)$ complete elliptic integral of the first kind

$K(\tau)$ complete elliptic integral of the second kind

r nondimensional radius vector in the rotor xy plane

R radius of vortex ring; radius of the rotor

R_P radial distance of a point P from the axis of a vortex ring (figure 1)

v normal component of the induced velocity at the center of the rotor

v_r radial component of the velocity induced at a point P by a vortex ring

v_z axial component of the velocity induced at a point P by a vortex ring

V velocity of helicopter along flight path

V_i normal component of the velocity induced at a point P by the whole wake

ΔV_i increment of the normal component of the velocity induced at a point P by that portion of the wake which is beyond the range of table I

w slope of the longitudinal variation of the nondimensional induced velocity in the plane of the rotor

W gross weight of the helicopter

x nondimensional radial distance of a point P from the axis of a vortex ring ($x = R_p/R$), (figure 1)

x', y', z' nondimensional coordinates of a point P with respect to rotor axes (figure 2)

X, Y, Z rotor axes (figure 3)

y slope of the lateral variation of the nondimensional induced velocity in the plane of the rotor

z nondimensional distance of a point P from the plane of a vortex ring, positive in the direction of v_z ($z = Z_p/R$), (figure 1)

Z_p distance of a point P from the plane of a vortex ring

α angle of attack of the plane of zero feathering

α_i induced angle of attack

α_f fuselage angle of attack

α_v angle of attack of the tip-path plane

β_o angle between radius vector from center of rotor to a point P lying in the xz plane, and the positive x axis, positive above rotor (figure 3)

Γ vortex strength

λ $(V \sin\alpha - v)/\Omega R$

λ_v $(V \sin\alpha_v - v)/\Omega R$

μ $V \cos\alpha /\Omega R$

μ_v $V \cos\alpha_v/\Omega R$

τ $\dfrac{d_2 - d_1}{d_2 + d_1}$

ϕ_c angle between flight path and horizontal plane, positive below horizontal

χ angle between axis of the wake and vertical rotor axis (figure 3)

ψ azimuth angle measured in xy plane between the radius vector to a point and the positive x axis, positive in going from positive x axis to positive y axis

Ω angular velocity of the rotor, rad/sec.

Subscripts:

B denotes values of the back rotor of two rotors in tandem

F denotes values of the front rotor of two rotors in tandem

v denotes values taken with respect to the virtual axis of rotation or to the tip-path plane

ANALYSIS

A. The Velocity Induced by a Vortex Ring

It is shown in reference 4 that the stream function at a point P (figure 1) in the flow field of a vortex ring of strength Γ and radius R may be expressed as

$$\psi = -\frac{\Gamma R}{2\pi}(d_1 + d_2)\left[K(\tau) - E(\tau)\right] \tag{1}$$

where R is the radius of the vortex ring, d_1R and d_2R are the least and greatest distances of the point P to the vortex ring,

$$\tau = \frac{d_2 - d_1}{d_2 + d_1} \tag{2}$$

and $K(\tau)$ and $E(\tau)$ are the complete elliptic integrals of the first and second kinds, respectively.

The flow field of a vortex ring is axially symmetric and thus the axial and radial velocity components, v_z and v_r, at a point P, having axial distance Z_P from the plane of the vortex ring and a radial distance R_P from the axis of symmetry, are given by

$$v_z = -\frac{1}{R_P}\frac{d\psi}{dR_P} \tag{3}$$

and

$$v_r = \frac{1}{R_P}\frac{d\psi}{dZ_P} \tag{4}$$

It is shown in reference 3 that equations 3 and 4 may be expressed as

$$v_z = \frac{\Gamma}{2\pi xR}(AB + CDF) \tag{5}$$

and

$$v_r = \frac{-\Gamma}{2\pi xR}(AB' + CDF') \tag{6}$$

where $A = K(\tau) - E(\tau)$ (7)

$$B = \frac{x - 1}{d_1} + \frac{x + 1}{d_2} \tag{8}$$

$$C = d_1 + d_2 \tag{9}$$

$$D = \frac{\tau E(\tau)}{1 - \tau^2} \tag{10}$$

$$F = 1 - \frac{(1 + x^2 + z^2) - d_1 d_2}{2 x^2} \cdot \frac{(1 + x)d_1^2 + (1 - x)d_2^2}{2x d_1 d_2} \tag{11}$$

$$B' = z\left[\frac{1}{d_1} + \frac{1}{d_2}\right] \tag{12}$$

$$F' = \frac{z}{x}\left[1 - \frac{1 + x^2 + z^2}{d_1 d_2}\right] \tag{13}$$

$$d_1 = \sqrt{z^2 + (x - 1)^2} \tag{14}$$

$$d_2 = \sqrt{z^2 + (x + 1)^2} \tag{15}$$

and $x = R_P/R$ = nondimensional radial distance of P from axis of vortex ring,

$z = Z_P/R$ = nondimensional distance of P from plane of vortex ring, taken positive in direction of v_z on ring axis.

The values of v_z and v_r given by equations 5 and 6 become indeterminate for points on the vortex ring axis where $x = 0$. In this case, it follows from the symmetry of the flow that the radial component of induced velocity is zero, and the axial component of induced velocity is shown in reference 5 to be

$$(v_z)_{x = 0} = \frac{-\Gamma}{2R}\left[\frac{1}{(1 + z^2)^{3/2}}\right] \tag{16}$$

Numerical values of $\frac{v_z R}{\Gamma}$, which is a nondimensional factor expressing the normal component of the induced velocity, v_z, in the vicinity of a vortex ring, are given in table I. The table includes a range of nondimensional axial distances of $-4.2 \leqq z \leqq 4.2$, and nondimensional radial distances of $0 \leqq x \leqq 5.0$. The increments of z at which the values of $\frac{v_z R}{\Gamma}$ are given are suitable for numerical integration by Simpson's rule. The tabulated values in the underlined columns were obtained by calculation; with the exception of those points which are close to the circumference of the vortex ring, they are accurate to four places. The remainder of the values in table I were obtained by interpolation.

B. The Normal Component of the Induced Velocity in the Vicinity of a Lifting Rotor

It was assumed in this report, as in references 1 and 2, that the rotor wake vortex distribution consists of a straight elliptic cylinder formed by a uniform distribution of an infinite number of vortex rings of infinitesimal strength, lying in planes parallel to the tip-path plane and extending downstream to infinity. The above-described vortex distribution is equivalent to a vortex sheet of uniform finite strength per unit length, $d\Gamma/dZ$, measured in the Z direction. This sheet forms a straight elliptic cylinder coinciding with the boundary of the wake.

Within the limitations of the initial assumptions, it may be shown from the results of references 1 and 2 that

$$\frac{d\Gamma}{dZ} = \frac{\Omega R\, C_T}{\lambda_v\left(1 - \frac{3}{2}\mu_v^2\right)} \approx \frac{\Omega R\, C_T}{\lambda\left(1 - \frac{3}{2}\mu^2\right)} \qquad (17)$$

where the subscript v denotes values with respect to tip-path plane coordinates.

The increment of the normal component of velocity at a point P in the vicinity of the rotor, induced by the wake vortex rings within the distance from P covered by table I, may thus be found by graphical or numerical integration. This increment constitutes about 95 per cent of the total value of the normal component at the center of the rotor and a large part of the total value for all points within the region considered in this paper.

The contribution of the vortex rings beyond the range of table I to the induced velocity at P may thus be summed, with small error in the final result, by an approximate expression which is integrable.

The value of the velocity potential $\Delta\phi_p$ at P due to a closed vortex element of strength Γ is shown in reference 6 to be

$$\Delta\phi_p = \frac{\Gamma}{4\pi}\omega \tag{18}$$

where ω = solid angle subtended at P by the closed vortex element.

It is a good approximation for those wake vortex rings at distances from P beyond the range of table I that the subtended solid angle at P is equal to three times that volume cut off the cone, determined by P and the ring, by a plane which is parallel to the plane of the ring and which is located a unit distance from P. It follows that

$$\Delta\phi_p \approx \frac{1}{4}\frac{d\Gamma}{dZ}\frac{z x^2 R\, dz}{(z^2 + x^2)^{3/2}} \tag{19}$$

Consequently, the increment to the normal component of velocity induced at P by that portion of the wake extending from the limit of table I, at

$z = z_1$, to $z = \infty$ may be obtained from the integral

$$\Delta V_i = \frac{1}{R}\frac{\partial \phi_P}{\partial z} = \frac{\partial}{\partial z}\int_{z_1}^{\infty} \frac{1}{4}\frac{d\Gamma}{dZ}\frac{z\,x^2\,dz}{(z^2 + x^2)^{3/2}} \tag{20}$$

It is shown in reference 3 that equation 20 may be integrated to obtain the value of ΔV_i at a point P having coordinates x', y', and z' from the center of the rotor, and that the result is

$$\Delta V_i = \frac{1}{2}\frac{d\Gamma}{dZ}\left[\left(\frac{2\sqrt{c}}{q} - \frac{2cz_2 + b}{q\sqrt{K}}\right)\left(1 - \frac{4ac + b^2}{cq}\right) + \frac{(b^2 - 2ac)\,z_2 + ab}{cq\,K^{3/2}}\right] \tag{21}$$

where $a = (x' - z' \tan\chi)^2 + y'^2$ (22)

$b = -2\,x' \tan\chi$ (23)

$c = 1 + \tan^2\chi$ (24)

$q = 4ac - b^2$ (25)

$K = a + b\,z_2 + c\,z_2^2$ (26)

and $z_2 = z_1 - z'$ (27)

For the point P (0,0,0) the value of ΔV_i given by equation 21 becomes indeterminate. It is possible, however, to substitute the zero coordinates in the equation before integrating. Doing so yields

$$(\Delta V_i)_{0,0,0} = -\frac{1}{8\,z_1^2}\frac{d\Gamma}{dZ}\cos^3\chi\,(3\cos^2\chi - 1) \tag{28}$$

The normal component of the induced velocity at any point $P(x',y',z')$ may thus be found in terms of $d\Gamma/dZ$ by adding the increment obtained from the numerical integration of the values induced by the

wake vortex rings within the range covered by table I to ΔV_i, obtained from equation 21 or 28.

It may be seen from figure 3 that, for $\chi < 90°$, or $\lambda_v = \lambda \cos a_1 + \mu \sin a_1 < 0$ or negative,

$$\chi = \tan^{-1}\left(\frac{-\mu_v}{\lambda_v}\right) = \tan^{-1}\left(\frac{-\mu}{\lambda}\right) + a_1 \tag{29}$$

and, for $\chi > 90°$, or $\lambda_v = \lambda \cos a_1 + \mu \sin a_1 > 0$ or positive,

$$\chi = \cot^{-1}\left(\frac{-\mu_v}{\lambda_v}\right) = \cot^{-1}\left(\frac{-\mu}{\lambda}\right) - a_1 \tag{30}$$

In the above equations a_1 is the coefficient of the cosine term of the Fourier series for the blade flapping angle

$$\beta = a_o - a_1 \cos\psi - b_1 \sin\psi - \ldots$$

where β is measured from the plane of zero feathering.

For $\chi = 90°$, equation 21 may be used by replacing $d\Gamma/dZ$ by its equivalent $(d\Gamma/dX) \tan\chi$, where, for $\chi = 90°$,

$$\frac{d\Gamma}{dX} = -\frac{\Omega R\, C_T}{\mu_v(1 - \frac{3}{2}\mu_v^2)} \approx -\frac{\Omega R\, C_T}{\mu(1 - \frac{3}{2}\mu^2)} \tag{31}$$

RESULTS

The results are presented in the form of tables and graphs of the ratio of the normal component of the induced velocity, V_i, at any point P $(\beta_P, X/R$ or $\beta_P, Y/R)$, as in Figure 3, to the normal component of the induced velocity v at the center of the rotor. It is shown in reference 2 that

$$v \approx \frac{\frac{1}{2}\Omega R\, C_T}{(1 - \frac{3}{2}\mu_v^2)\sqrt{\lambda_v^2 + \mu_v^2}} \approx \frac{\frac{1}{2}\Omega R\, C_T}{(1 - \mu^2)\sqrt{\lambda^2 + \mu^2}} \tag{32}$$

Consequently, the value of V_i at P may be easily computed from the values of V_i/v in the tables and graphs.

Table II gives the values of V_i/v for $-3.2 \leqq X/R \leqq 3.2$ and $\chi_p = \tan^{-1}(-1/2, -1/4, 0, 1/4, 1/2)$. Table III gives the values of V_i/v along the lateral axis of the tip-path plane. Figures 4 through 12 show the lines of constant values of V_i/v in the longitudinal plane of symmetry for wake angles having tangents of 0, 1/4, 1/2, 1, 2, 4, ∞, -4, and -2. Figures 13 and 14 show the variation of V_i/v with χ for points on the longitudinal and lateral axes of the tip-path plane.

APPLICATION OF RESULTS

A. The Determination of the Mean Value of the Normal Component of the Induced Velocity Over the Front and Back Rotors of a Tandem-Rotor Helicopter

Making the approximation that the mean values of the induced velocity are the values at the centers of the respective rotors, and being given the flight path velocity, climb angle, gross weight, fuselage drag, fuselage angle of attack, thrust and tip speed of the front and rear rotors and the geometry of the helicopter, the mean values of the induced velocities may be found as follows:

The angles of attack, α_v, of the tip-path planes of the front and rear rotors are very nearly

$$\alpha_v = \phi_c - \frac{D_f \cos \phi_c}{W - D_f \sin \phi_c} \tag{33}$$

where ϕ_c = angle between flight path and horizontal, positive below horizontal,

D_f = drag of fuselage

and W = gross weight.

Denote values of the parameters of the front rotor by the subscript F and of the back rotor by the subscript B.

Then

$$\mu_{v_F} = \left(\frac{V}{\Omega R}\right)_F \cos\alpha_v \tag{34}$$

and

$$\mu_{v_B} = \left(\frac{V}{\Omega R}\right)_B \cos\alpha_v \tag{35}$$

As a first approximation, the interference induced velocity at the front rotor due to the thrust of the back rotor may be neglected. Then

$$\lambda_{v_F} = \left(\frac{V}{\Omega R}\right)_F \sin\alpha_v - \frac{v_F}{(\Omega R)_F} \tag{36}$$

where the value of v_F is given by equation 32 or, for $\mu_{v_F} > 0.15$,

$$\frac{v}{\Omega R} \approx \frac{\frac{1}{2} C_T}{\mu_v \left(1 - \frac{3}{2}\mu_v^2\right)} \tag{37}$$

The value of χ_F may then be obtained from equations 29 or 30. When χ, α_v, α_f, v_F and the geometry of the helicopter are known, the position of the center of the rear rotor with respect to the front rotor can be determined. Then the nondimensional velocity, V_i/v, induced at the center of the rear rotor, because of the thrust of the front rotor, may be obtained by interpolation from one of figures 4 through 12 for the appropriate value of χ_F. The approximate value of $v_B$total is then

$$v_B\text{total} = (V_i/v)\, v_F + v_B \tag{38}$$

where v_B can be obtained from equations 33 or 37. The approximate values of λ_{v_B}, χ_B and, thus, the interference induced velocity at the front rotor may be found to evaluate v_F total. In general, it will be necessary to iterate v_B total for an accurate result, because of the rapid variation of the interference induced velocity at the rear rotor with change in the wake angle of the front rotor and with position of the rear rotor with respect to the tip-path plane of the front rotor.

For a tandem-rotor helicopter, having approximately equally loaded rotors of equal size spaced approximately a rotor diameter apart with small vertical offset and operating in the high speed flight range, it is seen from figures 9 and 10 that

$$\frac{v_F \text{total}}{\Omega R} \approx \frac{.47\ C_T}{\mu_v \left(1 - \frac{3}{2}\mu_v^2\right)} \tag{39}$$

and

$$\frac{v_B \text{total}}{\Omega R} \approx \frac{1.25\ C_T}{\mu_v \left(1 - \frac{3}{2}\mu_v^2\right)} \tag{40}$$

B. The Determination of the Longitudinal Variation of the Normal Component of the Induced Velocity over the Front and Back Rotors of a Tandem-Rotor Helicopter

If the normal component V_i of the induced velocity at $P(r, \psi)$ be approximated by the expression

$$\frac{V_i}{\Omega R} = -\frac{v}{\Omega R} + y\, r \sin\psi + w\, r \cos\psi \tag{41}$$

it may be shown from the results given in reference 2 that, for a single rotor,

$$w \approx -\frac{4}{3}\left[(1 - 1.8\mu_v^2)\sqrt{1 + \left(\frac{\lambda_v}{\mu_v}\right)^2} - \sqrt{\left(\frac{\lambda_v}{\mu_v}\right)^2}\right]\frac{v}{\Omega R} \qquad (42)$$

The increments in w arising from the second rotor of a tandem-rotor helicopter, to be added to the values given by equation 42 for the front and rear rotors, may be obtained in the general case from the values of V_i/v from the figures at $r = 0.75$ and $\psi = 0$ and π on the respective rotors. Thus,

$$\Delta w = -\left[\left(\frac{V_i}{v}\right)_{\substack{\psi = 0 \\ r = 0.75}} - \left(\frac{V_i}{v}\right)_{\substack{\psi = \pi \\ r = 0.75}}\right]\frac{2}{3}\frac{v}{\Omega R} \qquad (43)$$

For high-speed flight and small overlaps between the rotor disks

$$\Delta w_F \approx \frac{1}{6}\frac{v_B}{\Omega R} \qquad (44)$$

and, with less accuracy,

$$\Delta w_B \approx \frac{1}{4}\frac{v_F}{\Omega R} \qquad (45)$$

C. The Determination of the Induced Flow Angle at a Horizontal Tailplane

When the values of α_v, $\frac{v}{\Omega R}$, χ and α_f for the rotor or rotors in question have been determined and when the helicopter flight condition under consideration is known, the geometric position, and thus the values of Z/R and X/R, of the horizontal tailplane may be calculated, and the value or values of V_i/v found from the figures. Then the induced angle $\alpha_{i_{tail}}$ at the tailplane is approximately

$$\alpha_{i_{tail}} \approx -\frac{\left(\frac{V_i}{v}v\right)_F + \left(\frac{V_i}{v}v\right)_B}{V \cos \alpha_f} \qquad (46)$$

CONCLUDING DISCUSSION

The assumption that the planes of the wake vortex rings remain parallel to the tip-path plane is the only one of the various initial assumptions as to the wake distribution of vorticity which appears likely to affect the engineering accuracy of these results at the higher flight speeds. It is the opinion of the senior author that the present investigation and that of reference 1 indicate that the planes of the wake vortex rings must be tilted to the rear as they leave the rotor, possibly approaching a tilt angle in the ultimate wake of half the wake angle χ. The quantitative effects of such a tilting of the wake vortex rings may not be large, as the increments of the radial components of the induced velocity introduced because of the tilt of the wake vortex rings will tend to compensate for the decrease in the normal component.

At the center of the rotor, where the values of the induced velocity calculated by the method presented in this report could be compared with the values obtained from the exact integral, the error was in every case less than one per cent. However, for those points in the flow field that lie close to the wake vortex sheet, there are irregularities in the tabulated values of V_i/v caused by difficulties with the interpolations in the table of the values of the normal component of the induced velocity for the vortex rings.

In order to construct figures 4 through 14 it was necessary to compute a large number of values of V_i/v in addition to those listed in

table II. However, as these additional points were at scattered locations, and consequently of little use for any other purpose, they have been omitted from the Final Report.

Since the wake angles of the rotors of helicopters operating in the upper half of their speed range fall in a narrow band between 80 and 85 degrees, an attempt was made to compute the induced velocity distribution for a wake angle of approximately 82 degrees. These computations proved to be impractical unless a large number of additional values of the induced velocity of the vortex ring, for the region within two-tenths of a ring radius from the plane of the ring, were first computed. The additional labor did not appear to be justified because of the approximations involved in the initial assumptions.

It appears from the results of this investigation that the interference induced velocity at the rear rotor of a tandem-rotor helicopter in high-speed flight, due to the thrust of the front rotor, is of the same order of magnitude and of the same sign as the self-induced velocity. Consequently the interference induced velocity should be taken into account in longitudinal stability calculations and in computing the equilibrium values of the mean blade angle and torque coefficients. The interference induced velocity at the front rotor of a tandem-rotor helicopter in high-speed flight is of the order of seven per cent of the self-induced velocity and opposite in sign.

The longitudinal gradient of the interference induced velocities at both rotors of a tandem-rotor helicopter in high-speed flight is of opposite sign to the longitudinal gradients of the self-induced velocities,

and consequently will have the effect of reducing the required equilibrium values of b_1, the coefficient of the sine component of the flapping angle.

For side-by-side rotor helicopters in high-speed flight the mean values of the interference induced velocities are of the order of 15 per cent of the self-induced velocities and are opposite in sign. The lateral gradients of the mutual interference induced velocities are large for the adjacent portions of the rotors. These large gradients may cause early tip stall if the rotor rotation is such that the retreating blades are in this adjacent rotor position.

The normal component of the induced velocity inside the wake of a helicopter rotor in high-speed flight appears to reach its maximum and final value of about twice the value at the center of the rotor at a distance of about one rotor radius downstream. For hovering and the lower forward speeds the induced velocity inside the wake reaches its final value of about twice that at the center of the rotor at a distance of about two rotor radii downstream.

Prepared by _____
Walter Castles, Jr., Assoc. Prof.
Daniel Guggenheim School of
Aeronautics

Approved by _____
Donnell W. Dutton, Director
Daniel Guggenheim School of
Aeronautics

Approved by _____
Gerald A. Rosselot, Director
State Engineering Experiment
Station

REFERENCES

1. Coleman, Robert P., Feingold, Arnold M., and Stempin, Carl W.: Evaluation of the Induced Velocity Field of an Idealized Helicopter Rotor. WRL No. 126, NACA, 1945.

2. Meijer Drees, Jr.: A Theory of Airflow Through Rotors and its Application to some Helicopter Problems. The Journal of the Helicopter Association of Great Britain 3, No. 2, 79-104 (July-August-September 1949).

3. de Leeuw, Jacob Henri: The Normal Component of the Induced Velocity Near a Vortex Ring and its Application to Lifting Rotor Problems. Master's Thesis, Daniel Guggenheim School of Aeronautics, Georgia Institute of Technology, 1951.

4. Lamb, Horace: Hydrodynamics. Sixth Edition. Dover Publications, New York, 1945, Ch.VII, Sec. 161, p. 237.

5. Glauert, H.: On the Contraction of the Slipstream of an Airscrew. R and M 1067, British A.R.C., Feb. 1926.

6. Lamb, Horace: Hydrodynamics. Sixth Edition. Dover Publications, New York, 1945, Ch VII, Sec. 150, p.212.

APPENDIX

TABLE I--Section 1

NONDIMENSIONAL VALUES OF THE NORMAL COMPONENT OF THE INDUCED VELOCITY IN THE VICINITY OF A VORTEX RING

$\frac{v_z R}{\Gamma}$

$z = \frac{\pm Z_P}{R}$	$x = \frac{R_P}{R} =$ 0.0	0.1	0.2	0.3	0.4	0.5	0.6
0.0	0.5000	0.5038	0.5156	0.5369	0.5707	0.6228	0.7053
0.1	0.4926	0.4961	0.5070	0.5264	0.5569	0.6025	0.6711
0.2	0.4714	0.4712	0.4827	0.4974	0.5193	0.5494	0.5881
0.4	0.4002	0.4010	0.4032	0.4064	0.4093	0.4098	0.4034
0.6	0.3153	0.3147	0.3128	0.3089	0.3022	0.2911	0.2735
0.8	0.2381	0.2370	0.2338	0.2281	0.2196	0.2076	0.1919
1.0	0.1768	0.1758	0.1728	0.1677	0.1604	0.1508	0.1391
1.3	0.1133	0.1127	0.1106	0.1073	0.1027	0.0969	0.0900
1.6	0.0744	0.0740	0.0728	0.0708	0.0681	0.0647	0.0608
2.1	0.0397	0.0396	0.0391	0.0382	0.0371	0.0357	0.0341
2.6	0.0231	0.0231	0.0228	0.0225	0.0220	0.0213	0.0206
3.4	0.0112	0.0112	0.0111	0.0110	0.0109	0.0106	0.0104
4.2	0.0062	0.0062	0.0062	0.0061	0.0061	0.0060	0.0059

Note: Values in underlined columns were obtained by calculation, the others by interpolation.

TABLE I--Section 2

NONDIMENSIONAL VALUES OF THE NORMAL COMPONENT OF THE INDUCED VELOCITY IN THE VICINITY OF A VORTEX RING

	$\frac{v_z R}{\Gamma}$						
$x = \frac{R_p}{R} =$	0.7	0.8	0.9	1.0	1.1	1.2	1.3
$z = \frac{\pm Z_p}{R}$							
0.0	0.8461	1.1293	1.9630	—	-1.2627	-0.5324	-0.3062
0.1	0.7768	0.9397	1.0938	0.2687	-0.5298	-0.3951	-0.2633
0.2	0.6304	0.6496	0.5501	0.2126	-0.1094	-0.1941	-0.1756
0.4	0.3825	0.3365	0.2568	0.1550	+0.0574	-0.0096	-0.0438
0.6	0.2476	0.2121	0.1682	0.1201	0.0747	+0.0371	+0.0099
0.8	0.1721	0.1486	0.1225	0.0956	0.0698	0.0470	0.0284
1.0	0.1253	0.1099	0.0934	0.0768	0.0607	0.0460	0.0332
1.3	0.0822	0.0738	0.0649	0.0560	0.0473	0.0391	0.0316
1.6	0.0563	0.0516	0.0465	0.0415	0.0364	0.0315	0.0269
2.1	0.0322	0.0302	0.0281	0.0259	0.0236	0.0209	0.0192
2.6	0.0197	0.0188	0.0178	0.0168	0.0156	0.0146	0.0135
3.4	0.0101	0.0098	0.0095	0.0091	0.0087	0.0083	0.0079
4.2	0.0058	0.0056	0.0055	0.0054	0.0052	0.0050	0.0048

Note: Values in underlined columns were obtained by calculation, the others by interpolation.

TABLE I--Section 3

NONDIMENSIONAL VALUES OF THE NORMAL COMPONENT OF THE INDUCED VELOCITY IN THE VICINITY OF A VORTEX RING

	$\frac{v_z R}{\Gamma}$						
$x = \frac{R_p}{R} =$	1.4	1.5	1.6	1.7	1.8	1.9	2.0
$z = \frac{\pm Z_p}{R}$							
0.0	-0.2010	-0.1424	-0.1060	-0.0817	-0.0647	-0.0524	-0.0431
0.1	-0.1833	-0.1336	-0.1011	-0.0788	-0.0629	-0.0511	-0.0423
0.2	-0.1411	-0.1112	-0.0882	-0.0709	-0.0577	-0.0477	-0.0398
0.4	-0.0559	-0.0567	-0.0527	-0.0471	-0.0414	-0.0362	-0.0315
0.6	-0.0076	-0.0175	-0.0218	-0.0241	-0.0241	-0.0230	-0.0215
0.8	+0.0141	+0.0038	-0.0031	-0.0076	-0.0103	-0.0117	-0.0122
1.0	0.0226	0.0141	+0.0073	+0.0026	-0.0009	-0.0034	-0.0050
1.3	0.0249	0.0190	0.0141	0.0100	+0.0067	+0.0040	+0.0020
1.6	0.0226	0.0187	0.0153	0.0122	0.0096	0.0074	0.0060
2.1	0.0171	0.0151	0.0132	0.0115	0.0099	0.0085	0.0072
2.6	0.0124	0.0113	0.0103	0.0093	0.0084	0.0075	0.0067
3.4	0.0075	0.0070	0.0066	0.0062	0.0058	0.0054	0.0050
4.2	0.0047	0.0045	0.0043	0.0041	0.0039	0.0037	0.0035

Note: Values in underlined columns were obtained by calculation, the others by interpolation.

TABLE I—Section 4

NONDIMENSIONAL VALUES OF THE NORMAL COMPONENT OF THE INDUCED VELOCITY IN THE VICINITY OF A VORTEX RING

	$\frac{v_z R}{\Gamma}$						
$x = \frac{R_p}{R} =$	2.1	2.2	2.3	2.4	2.5	2.6	2.7
$z = \frac{\pm Z_p}{R}$							
0.0	-0.0358	-0.0300	-0.0254	-0.0219	-0.0191	-0.0170	-0.0151
0.1	-0.0350	-0.0292	-0.0250	-0.0216	-0.0189	-0.0169	-0.0150
0.2	-0.0334	-0.0283	-0.0241	-0.0209	-0.0183	-0.0164	-0.0146
0.4	-0.0272	-0.0238	-0.0208	-0.0183	-0.0164	-0.0147	-0.0132
0.6	-0.0199	-0.0181	-0.0163	-0.0149	-0.0136	-0.0123	-0.0112
0.8	-0.0121	-0.0119	-0.0115	-0.0108	-0.0101	-0.0095	-0.0089
1.0	-0.0056	-0.0059	-0.0062	-0.0067	-0.0068	-0.0067	-0.0066
1.3	+0.0008	-0.0006	-0.0016	-0.0022	-0.0029	-0.0032	-0.0034
1.6	0.0045	+0.0031	+0.0021	+0.0012	+0.0002	-0.0005	-0.0009
2.1	0.0062	0.0052	0.0043	0.0035	0.0028	+0.0020	+0.0015
2.6	0.0059	0.0052	0.0046	0.0040	0.0034	0.0029	0.0025
3.4	0.0046	0.0042	0.0039	0.0036	0.0033	0.0030	0.0027
4.2	0.0033	0.0031	0.0029	0.0027	0.0025	0.0024	0.0023

Note: Values in underlined columns were obtained by calculation, the others by interpolation.

TABLE I--Section 5

NONDIMENSIONAL VALUES OF THE NORMAL COMPONENT OF THE INDUCED VELOCITY IN THE VICINITY OF A VORTEX RING

	$\frac{v_z R}{\Gamma}$						
$x = \frac{R_p}{R} =$	2.8	2.9	3.0	3.1	3.2	3.3	3.4
$z = \frac{\pm Z_p}{R}$							
0.0	-0.0135	-0.0121	-0.0109	-0.0097	-0.0086	-0.0077	-0.0070
0.1	-0.0133	-0.0120	-0.0108	-0.0096	-0.0085	-0.0076	-0.0069
0.2	-0.0129	-0.0117	-0.0105	-0.0095	-0.0084	-0.0075	-0.0068
0.4	-0.0119	-0.0107	-0.0098	-0.0089	-0.0079	-0.0072	-0.0065
0.6	-0.0102	-0.0094	-0.0087	-0.0079	-0.0071	-0.0065	-0.0059
0.8	-0.0082	-0.0076	-0.0070	-0.0065	-0.0061	-0.0056	-0.0051
1.0	-0.0063	-0.0061	-0.0058	-0.0054	-0.0050	-0.0047	-0.0044
1.3	-0.0036	-0.0038	-0.0037	-0.0036	-0.0034	-0.0032	-0.0031
1.6	-0.0012	-0.0016	-0.0017	-0.0018	-0.0019	-0.0019	-0.0019
2.1	+0.0011	+0.0007	+0.0004	+0.0001	-0.0001	-0.0003	-0.0004
2.6	0.0022	0.0019	0.0016	0.0013	+0.0010	+0.0008	+0.0007
3.4	0.0024	0.0021	0.0019	0.0017	0.0016	0.0014	0.0013
4.2	0.0022	0.0021	0.0020	0.0019	0.0019	0.0017	0.0016

Notes: Values in underlined columns were obtained by calculation, the others by interpolation.

TABLE I--Section 6

NONDIMENSIONAL VALUES OF THE NORMAL COMPONENT OF THE INDUCED VELOCITY IN THE VICINITY OF A VORTEX RING

	$\frac{v_z R}{\Gamma}$						
$x = \frac{R_p}{R} =$	3.5	3.6	3.7	3.8	3.9	4.0	4.1
$z = \frac{\pm Z_p}{R}$							
0.0	-0.0064	-0.0058	-0.0053	-0.0049	-0.0045	-0.0042	-0.0039
0.1	-0.0063	-0.0058	-0.0053	-0.0049	-0.0045	-0.0042	-0.0039
0.2	-0.0062	-0.0057	-0.0052	-0.0048	-0.0044	-0.0041	-0.0038
0.4	-0.0060	-0.0055	-0.0051	-0.0047	-0.0043	-0.0040	-0.0037
0.6	-0.0054	-0.0050	-0.0046	-0.0043	-0.0040	-0.0037	-0.0035
0.8	-0.0047	-0.0044	-0.0041	-0.0039	-0.0036	-0.0034	-0.0032
1.0	-0.0041	-0.0038	-0.0036	-0.0034	-0.0032	-0.0030	-0.0028
1.3	-0.0029	-0.0028	-0.0027	-0.0026	-0.0025	-0.0024	-0.0022
1.6	-0.0020	-0.0019	-0.0019	-0.0019	-0.0018	-0.0018	-0.0017
2.1	-0.0005	-0.0006	-0.0007	-0.0008	-0.0008	-0.0009	-0.0009
2.6	+0.0005	+0.0003	+0.0002	+0.0001	0.0000	-0.0001	-0.0002
3.4	0.0011	0.0010	0.0009	0.0007	0.0006	0.0005	+0.0004
4.2	0.0015	0.0014	0.0012	0.0011	0.0010	0.0009	0.0008

Note: Values in underlined columns were obtained by calculation, the others by interpolation.

TABLE I--Section 7

NONDIMENSIONAL VALUES OF THE NORMAL COMPONENT OF THE INDUCED VELOCITY IN THE VICINITY OF A VORTEX RING

	$\frac{v_z R}{\Gamma}$						
$x = \frac{R_P}{R} =$	4.2	4.3	4.4	4.5	4.6	4.7	4.8
$z = \frac{\pm Z_P}{R}$							
0.0	-0.0037	-0.0034	-0.0032	-0.0030	-0.0028	-0.0026	-0.0024
0.1	-0.0037	-0.0034	-0.0032	-0.0030	-0.0028	-0.0026	-0.0024
0.2	-0.0036	-0.0033	-0.0031	-0.0029	-0.0027	-0.0025	-0.0024
0.4	-0.0035	-0.0032	-0.0030	-0.0028	-0.0026	-0.0024	-0.0023
0.6	-0.0033	-0.0030	-0.0029	-0.0027	-0.0025	-0.0023	-0.0022
0.8	-0.0030	-0.0028	-0.0026	-0.0025	-0.0023	-0.0022	-0.0020
1.0	-0.0026	-0.0025	-0.0023	-0.0022	-0.0021	-0.0020	-0.0019
1.3	-0.0021	-0.0020	-0.0020	-0.0019	-0.0018	-0.0017	-0.0017
1.6	-0.0017	-0.0016	-0.0015	-0.0015	-0.0015	-0.0014	-0.0014
2.1	-0.0009	-0.0009	-0.0009	-0.0009	-0.0009	-0.0009	-0.0009
2.6	-0.0003	-0.0004	-0.0004	-0.0005	-0.0005	-0.0005	-0.0005
3.4	+0.0003	+0.0002	+0.0002	+0.0001	+0.0001	0.0000	0.0000
4.2	0.0007	0.0006	0.0005	0.0005	0.0004	0.0004	0.0003

Note: Values in underlined columns were obtained by calculation, the others by interpolation.

TABLE I—Section 8

NONDIMENSIONAL VALUES OF THE NORMAL COMPONENT OF THE INDUCED VELOCITY IN THE VICINITY OF A VORTEX RING

	$\frac{v_z R}{\Gamma}$	
$x = \frac{R_P}{R} =$	4.9	5.0
$z = \frac{\pm Z_P}{R}$		
0.0	-0.0022	-0.0021
0.1	-0.0022	-0.0021
0.2	-0.0022	-0.0021
0.4	-0.0021	-0.0020
0.6	-0.0021	-0.0020
0.8	-0.0019	-0.0018
1.0	-0.0018	-0.0017
1.3	-0.0016	-0.0015
1.6	-0.0013	-0.0013
2.1	-0.0009	-0.0008
2.6	-0.0005	-0.0005
3.4	0.0000	0.0000
4.2	0.0003	0.0002

Note: Values in underlined columns were obtained by calculation, the others by interpolation.

TABLE II

NONDIMENSIONAL VALUES OF THE NORMAL COMPONENT OF THE INDUCED VELOCITY IN THE LONGITUDINAL PLANE OF SYMMETRY OF A LIFTING ROTOR FOR $\chi \leq 90°$

For the flight conditions for which $\chi > 90°$ and a developed wake exists, the values of V_i/v for the condition $(\chi, X/R, \beta_p)$ are the same as for the condition $(180° - \chi, X/R, -\beta_p)$.

Section 1

V_i/v for $\chi = 0°$					
	$\tan\beta_p$				
X/R	-1/2	-1/4	0	1/4	1/2
0.00	1.000	1.000	1.000	1.000	1.000
0.40	1.220	1.112	1.000	0.888	0.780
0.80	1.555	1.368	1.000	0.632	0.445
0.90	1.643	1.495	1.000	0.505	0.357
1.00	---	---	0.500	0.363	0.282
1.10	-0.224	-0.253	0.000	0.253	0.224
1.20	-0.180	-0.180	0.000	0.180	0.180
1.60	-0.088	-0.067	0.000	0.067	0.088
2.00	-0.053	-0.038	0.000	0.038	0.053
3.20	-0.019	-0.012	0.000	0.012	0.019

Notes: 1. Value of V_i/v changes 2.000 units in passing through boundary of the wake.

2. Values of V_i/v are axially symmetric about rotor axis.

3. Values of V_i/v are anti-symmetric about the tip-path plane, and the value about which they are anti-symmetric is 1.000 for $X/R < 1$ and 0.000 for $X/R > 1$.

TABLE II--Section 2

V_i/v for $\chi = 14.04°$ ($\tan\chi = 1/4$)					
	$\tan\beta_P$				
X/R	-1/2	-1/4	0	1/4	1/2
-3.20	0.011	0.001	-0.010	-0.020	-0.023
-2.00	0.028	0.012	-0.027	-0.061	-0.063
-1.60	0.057	0.026	-0.046	-0.101	-0.105
-1.20	0.132	0.099	-0.108	-0.232	-0.200
-0.80	0.363	0.521	0.860	1.245	1.406
-0.40	0.729	0.835	0.948	1.059	1.170
0.00	1.000	1.000	1.000	1.000	1.000
0.40	1.262	1.161	1.052	0.940	0.828
0.80	1.626	1.479	1.139	0.746	0.526
1.20	---	-0.036	0.150	0.281	0.242
1.60	---	0.004	0.079	0.121	0.126
2.00	-0.013	0.007	0.046	0.073	0.077
3.20	-0.001	0.004	0.016	0.034	0.028
1.40	-0.042	---	---	---	---

Note: Value of V_i/v changes 1.940 units in passing through boundary of the wake.

TABLE II--Section 3

V_i/v for $\chi = 26.56°$ ($\tan\chi = 1/2$)					
	$\tan\beta_p$				
X/R	-1/2	-1/4	0	1/4	1/2
-3.20	0.005	-0.004	-0.016	-0.024	-0.026
-2.00	0.019	-0.006	-0.044	-0.067	-0.065
-1.60	0.034	-0.016	-0.073	-0.120	-0.109
-1.20	0.089	0.038	-0.180	-0.261	-0.198
-0.80	0.305	0.426	0.738	---	---
-0.40	0.687	0.788	0.899	1.046	1.126
0.00	1.000	1.000	1.000	1.000	1.000
0.40	1.314	1.211	1.101	0.987	0.874
0.80	1.692	1.582	1.261	0.860	0.604
1.20	1.803	---	0.328	0.403	0.305
1.60	0.113	0.125	0.167	0.191	0.166
2.00	0.088	0.084	0.105	0.115	0.105
3.20	0.038	0.037	0.041	0.044	0.040

Note: Value of V_i/v changes 1.789 units in passing through boundary of the wake.

TABLE II--Section 4

V_i/v for $\chi = 45.00°$ ($\tan\chi = 1$)					
	$\tan\beta_P$				
X/R	-1/2	-1/4	0	1/4	1/2
-3.20	-0.002	-0.010	-0.019	-0.025	-0.023
-2.00	-0.001	-0.028	-0.060	-0.071	-0.060
-1.60	0.006	-0.039	-0.107	-0.122	-0.096
-1.20	0.036	-0.039	-0.265	-0.249	-0.172
-0.80	0.217	0.285	0.535	---	-0.142
-0.40	0.622	0.719	0.824	0.927	1.046
0.00	1.000	1.000	1.000	1.000	1.000
0.40	1.381	1.283	1.176	1.062	0.947
0.80	1.782	1.711	1.465	1.048	0.740
1.20	1.957	1.866	0.683	0.593	0.423
1.60	1.829	0.467	0.410	0.332	0.247
2.00	---	0.372	0.272	0.215	0.164
3.20	0.307	0.165	0.113	0.087	0.066

Note: Value of V_i/v changes 1.414 units in passing through boundary of the wake.

TABLE II--Section 5

V_i/v for $\chi = 63.43°$ ($\tan\chi = 2$)					
	$\tan\beta_p$				
X/R	-1/2	-1/4	0	1/4	1/2
-3.20	-0.008	-0.021	-0.022	-0.020	-0.020
-2.00	-0.015	-0.043	-0.064	-0.069	-0.051
-1.60	-0.020	-0.067	-0.119	-0.116	-0.083
-1.20	-0.012	-0.105	-0.294	-0.238	-0.140
-0.80	0.124	0.140	0.326	-0.320	-0.144
-0.40	0.550	0.639	0.746	0.858	---
0.00	1.000	1.000	1.000	1.000	1.000
0.40	1.460	1.366	1.254	1.144	1.032
0.80	1.886	1.849	1.674	1.265	0.911
1.20	2.022	2.098	1.240	0.900	0.600
1.60	2.030	2.098	0.878	0.582	0.384
2.00	2.026	---	0.653	0.401	0.262
3.20	2.017	0.776	0.278	0.181	0.100

Note: Value of V_i/v changes 0.894 units in passing through boundary of the wake.

TABLE II--Section 6

V_i/v for $\chi = 75.97°$ ($\tan\chi = 4$)					
	$\tan\beta_P$				
X/R	-1/2	-1/4	0	1/4	1/2
-3.20	-0.011	-0.019	-0.026	-0.022	-0.014
-2.00	-0.025	-0.052	-0.072	-0.065	-0.043
-1.60	-0.035	-0.084	-0.124	-0.101	-0.067
-1.20	-0.043	-0.136	-0.309	-0.213	-0.110
-0.80	0.062	0.054	0.166	-0.193	-0.087
-0.40	0.485	0.549	0.675	---	0.483
0.00	1.000	1.000	1.000	1.000	1.000
0.40	1.494	1.427	1.325	1.165	1.096
0.80	1.576	1.942	1.834	1.436	1.053
1.20	1.895	2.150	---	1.183	0.763
1.60	1.250	2.086	1.384	0.869	0.530
2.00	0.967	2.063	1.187	0.623	0.377
3.20	0.735	2.022	0.785	0.328	0.169

Note: Value of V_i/v changes 0.485 units in passing through boundary of the wake.

TABLE II--Section 7

V_i/v for $\chi = 90.00°$					
	$\tan\beta_P$				
X/R	-1/2	-1/4	0	1/4	1/2
-3.20	-0.016	-0.022	-0.026	-0.022	-0.016
-2.00	-0.035	-0.060	-0.078	-0.060	-0.035
-1.60	-0.052	-0.097	-0.137	-0.097	-0.052
-1.20	-0.076	-0.182	-0.331	-0.182	-0.076
-0.80	-0.010	-0.057	-0.075	-0.057	-0.010
-0.40	0.414	0.519	0.564	0.519	0.414
0.00	1.000	1.000	1.000	1.000	1.000
0.40	1.193	1.312	1.436	1.312	1.193
0.80	1.266	1.664	2.075	1.664	1.266
1.20	1.046	1.602	2.331	1.602	1.046
1.60	0.804	1.354	2.137	1.354	0.804
2.00	0.619	1.175	2.078	1.175	0.619
3.20	0.318	0.774	2.026	0.774	0.318
-1.00	---	---	-0.621	---	---

Note: 1. Values of V_i/v are symmetric about the tip-path plane.

2. Values of V_i/v for $\beta_P = 0$ are anti-symmetric about a value of $V_i/v = 1$ at $X = 0$.

3. Values of V_i/v for $\beta_P = 0$ were obtained by extrapolation.

TABLE III

NONDIMENSIONAL VALUES OF THE NORMAL COMPONENT OF THE INDUCED VELOCITY ON THE LATERAL AXIS OF A LIFTING ROTOR

V_i/v					
	tan χ				
±Y/R	0	1	2	4	∞
0.00	1.000	1.000	1.000	1.000	1.000
0.40	1.000	1.000	1.000	1.000	1.000
0.60	1.000	---	---	---	0.978
0.80	1.000	---	---	---	0.904
1.10	1.000	---	-0.702	-1.071	-1.399
1.20	0.000	-0.235	-0.548	-0.693	-0.809
1.40	0.000	-0.158	-0.319	-0.401	-0.428
1.60	0.000	-0.114	-0.239	-0.256	-0.281
2.00	0.000	-0.068	-0.119	-0.144	-0.154
3.20	0.000	-0.026	-0.041	-0.049	-0.053

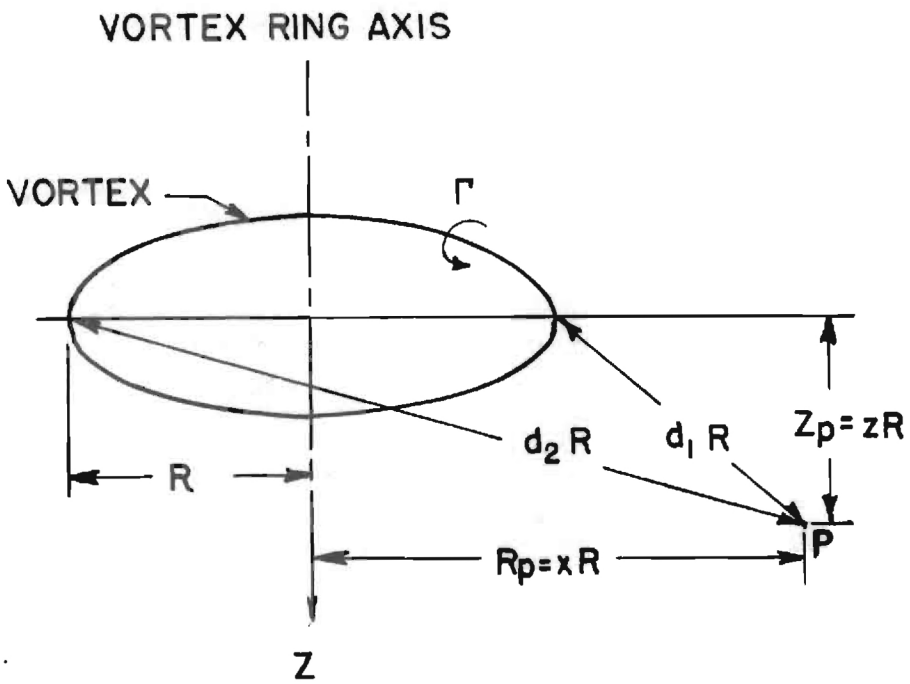

Figure 1. Coordinates for Vortex Ring and Table I.

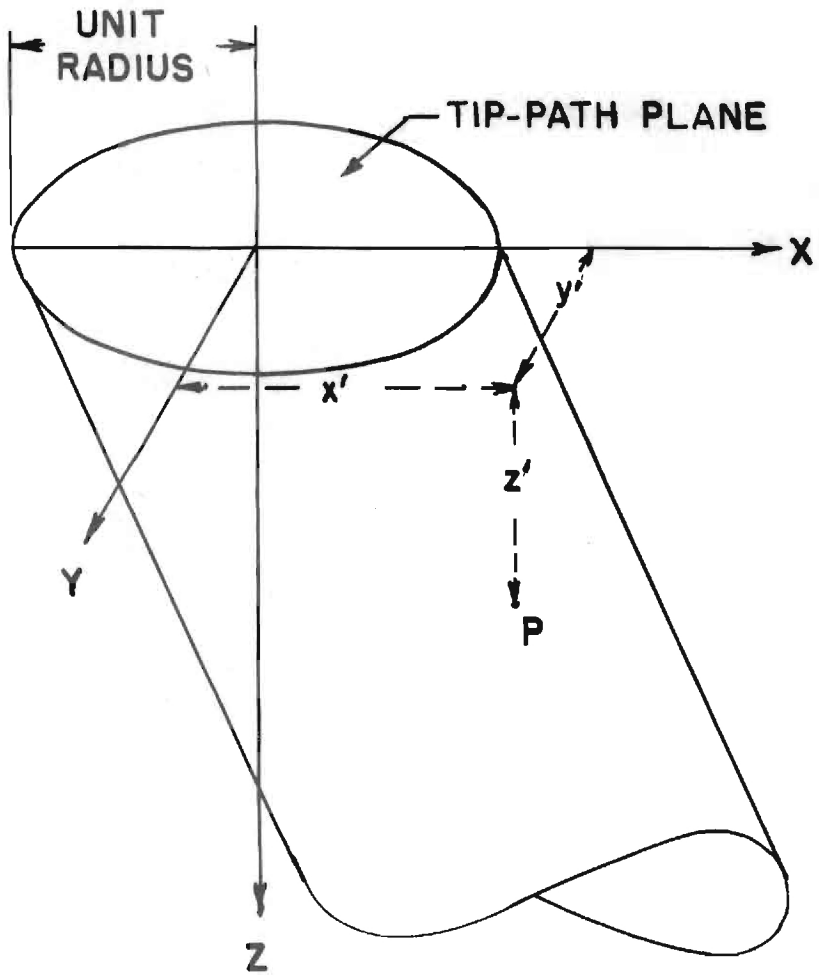

Figure 2. Nondimensional Rotor Coordinates.

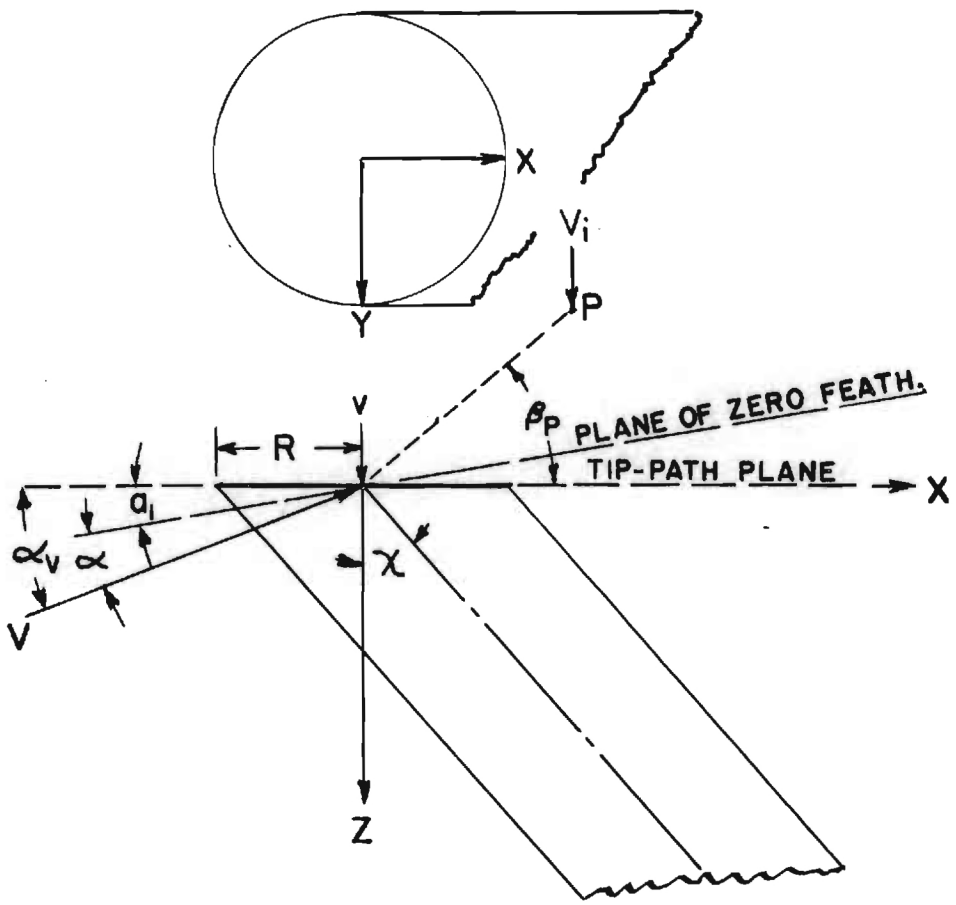

Figure 3. Geometry of Wake.

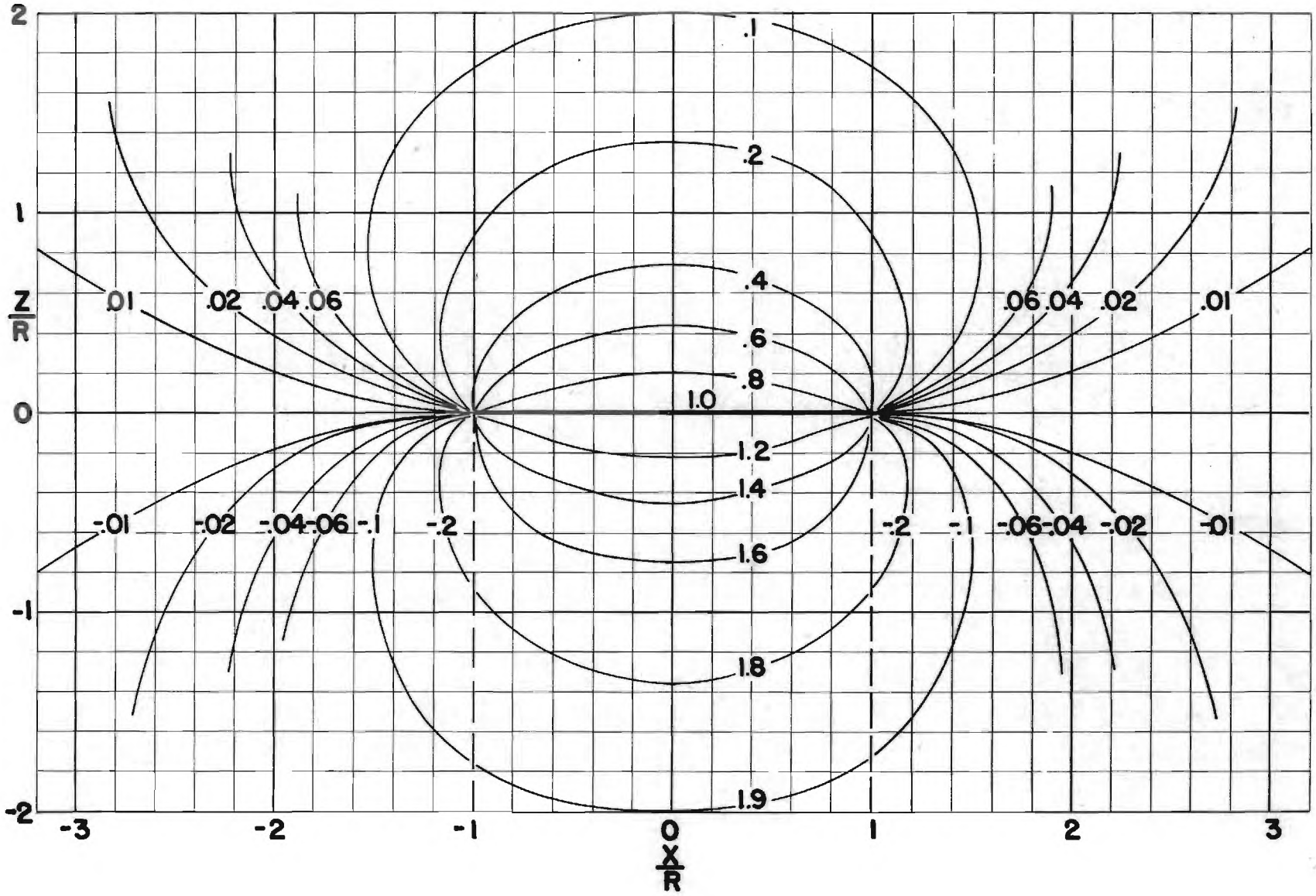

Figure 4. ISO-Induced Velocity Lines for X = 0° = TAN^{-1} 0

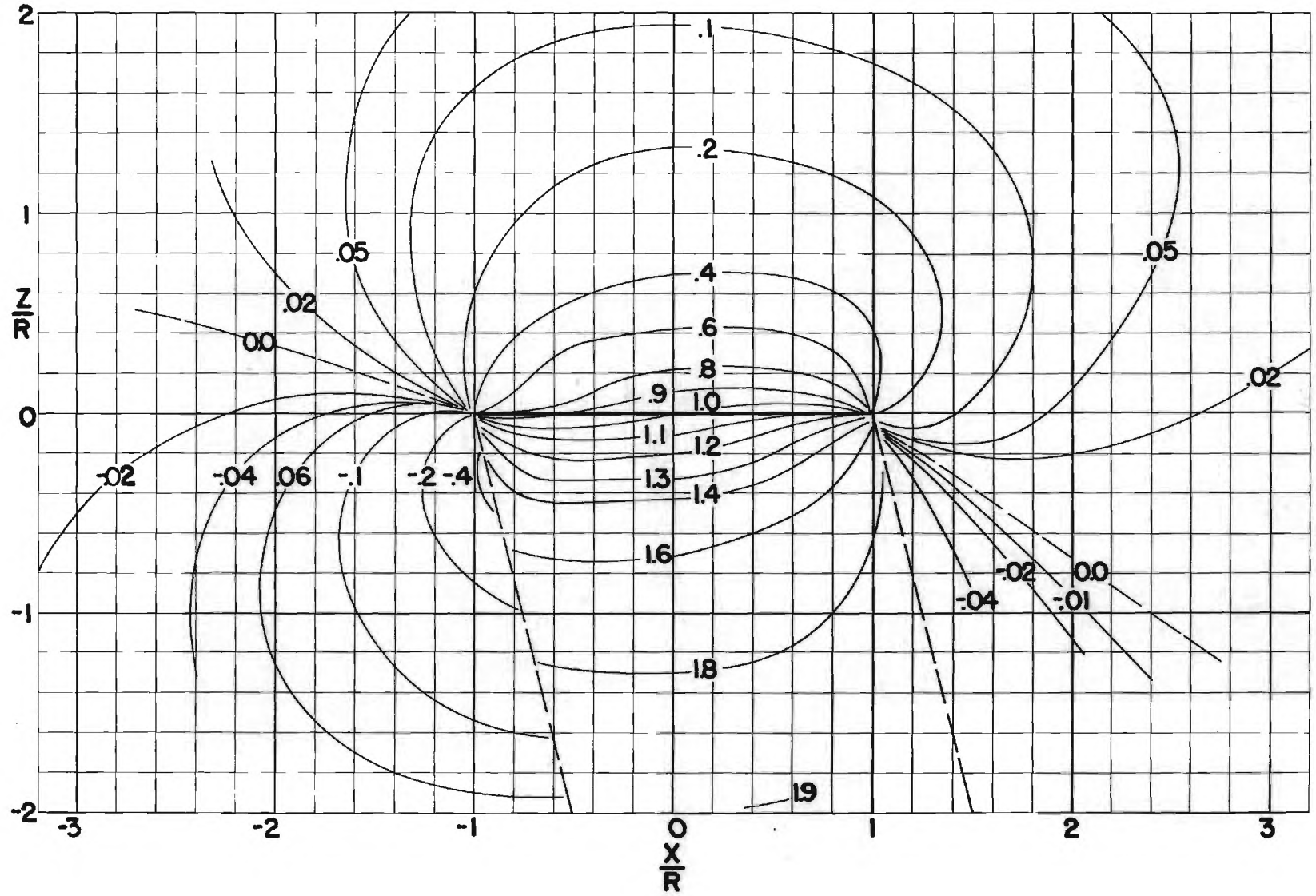

Figure 5. ISO-Induced Velocity Lines ror X = 13.0° = TAN^{-1} ¼.

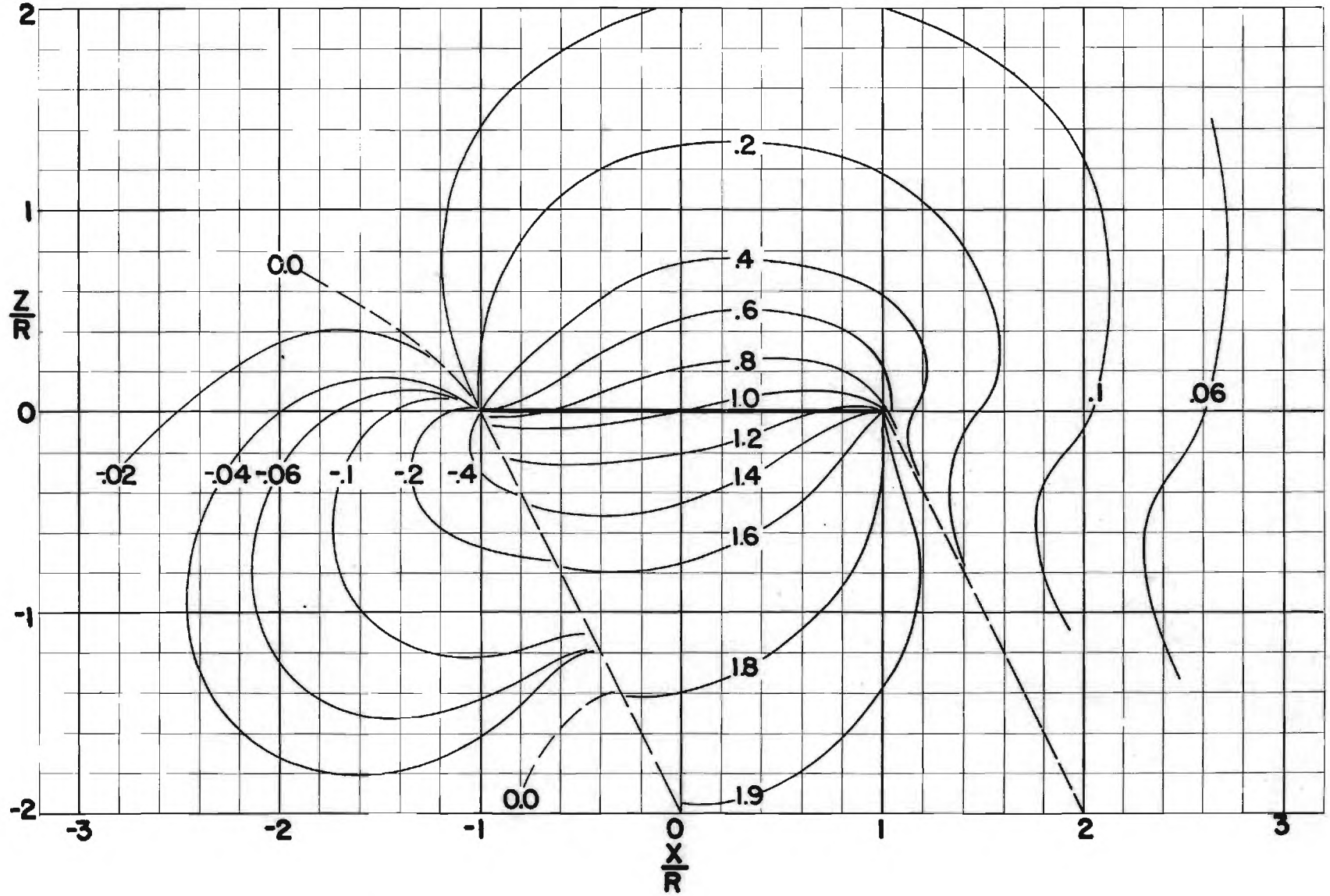

Figure 6. ISO-Induced Velocity Lines for X = 26.5° = TAN^{-1} ½.

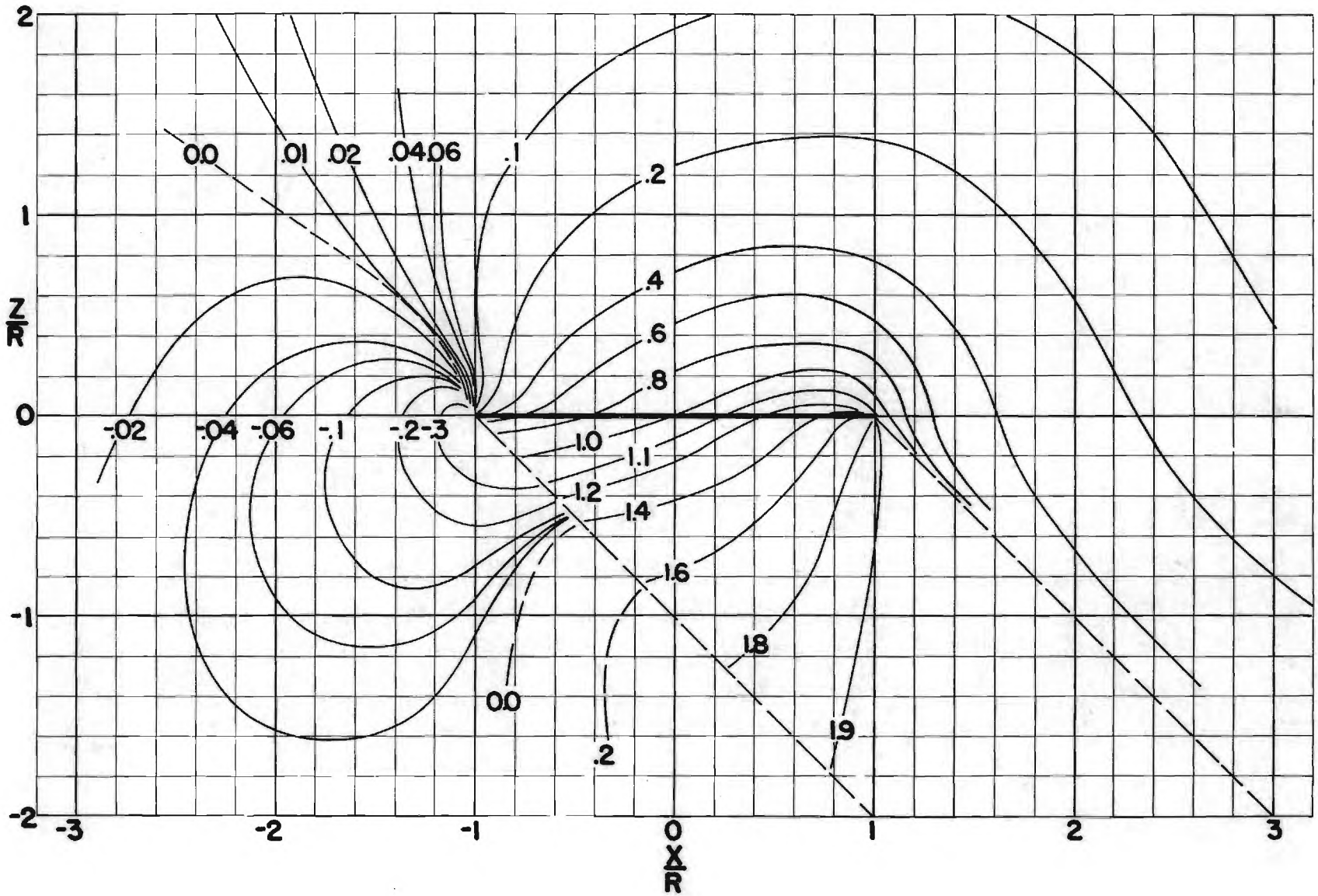

Figure 7. ISO-Induced Velocity Lines for X = 45.0° = TAN^{-1} 1.

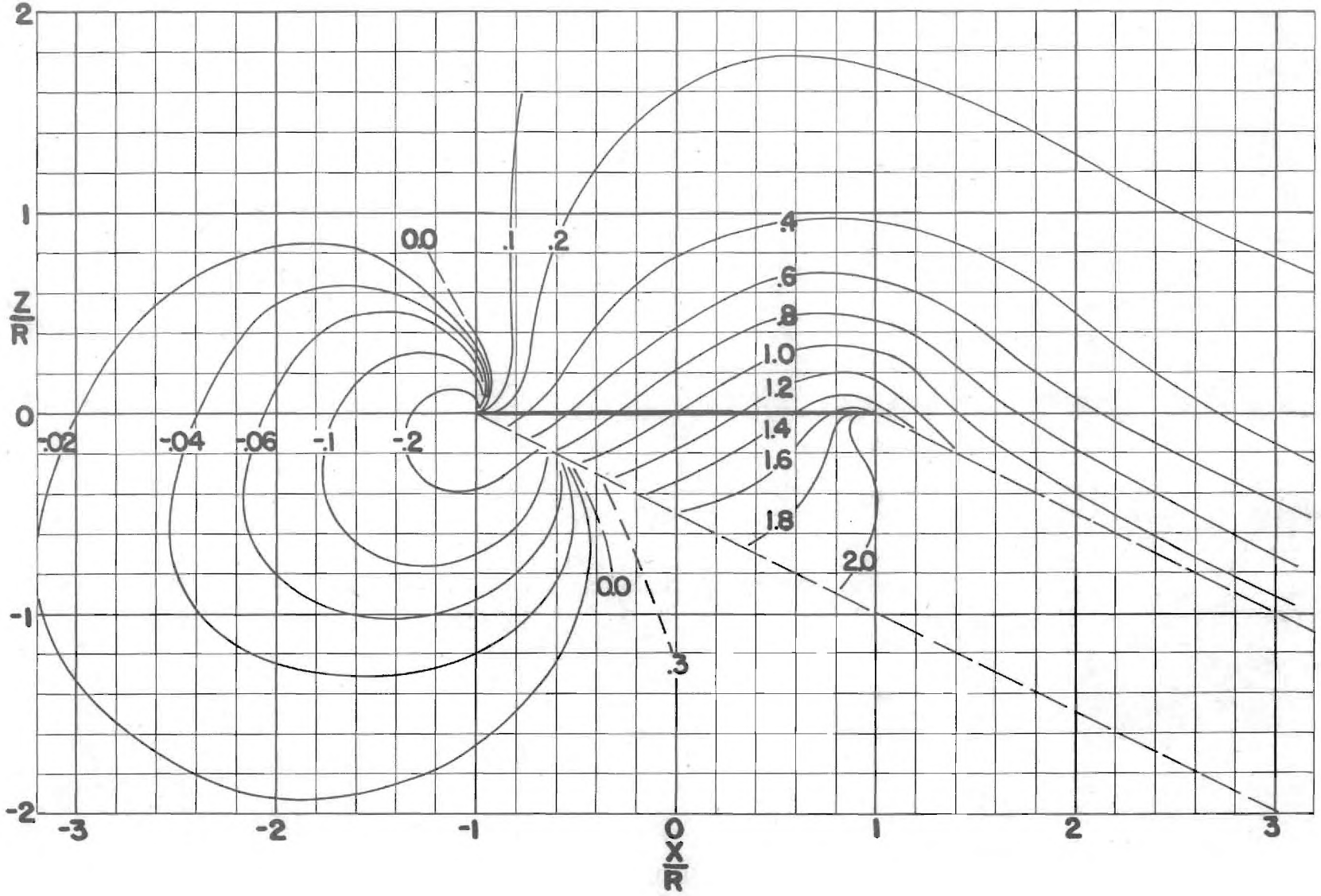

Figure 8. ISO-Induced Velocity Lines for X = 63.4° = TAN^{-1} 2.

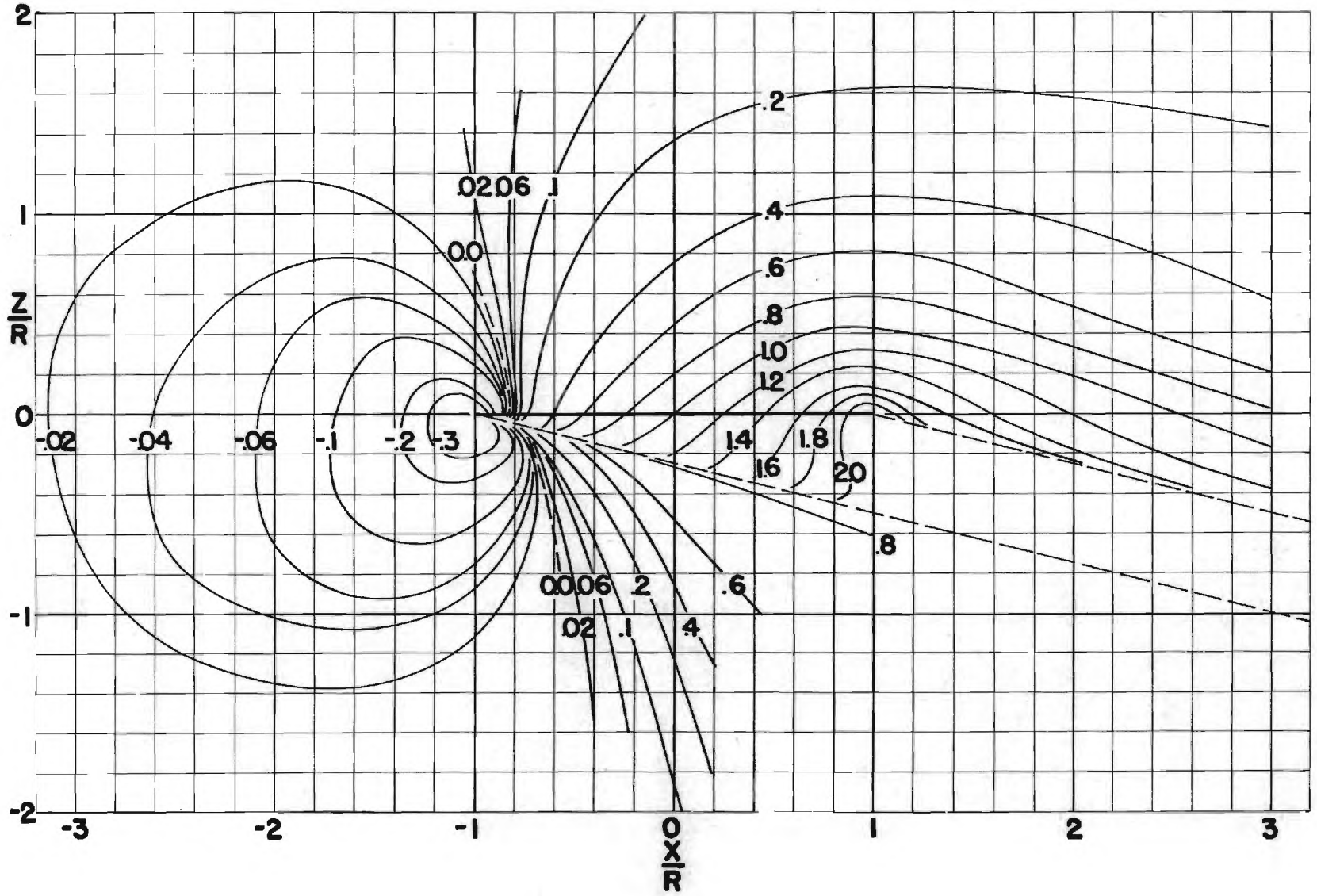

Figure 9. ISO-Induced Velocity Lines for X = 76.0° = TAN^{-1} 4.

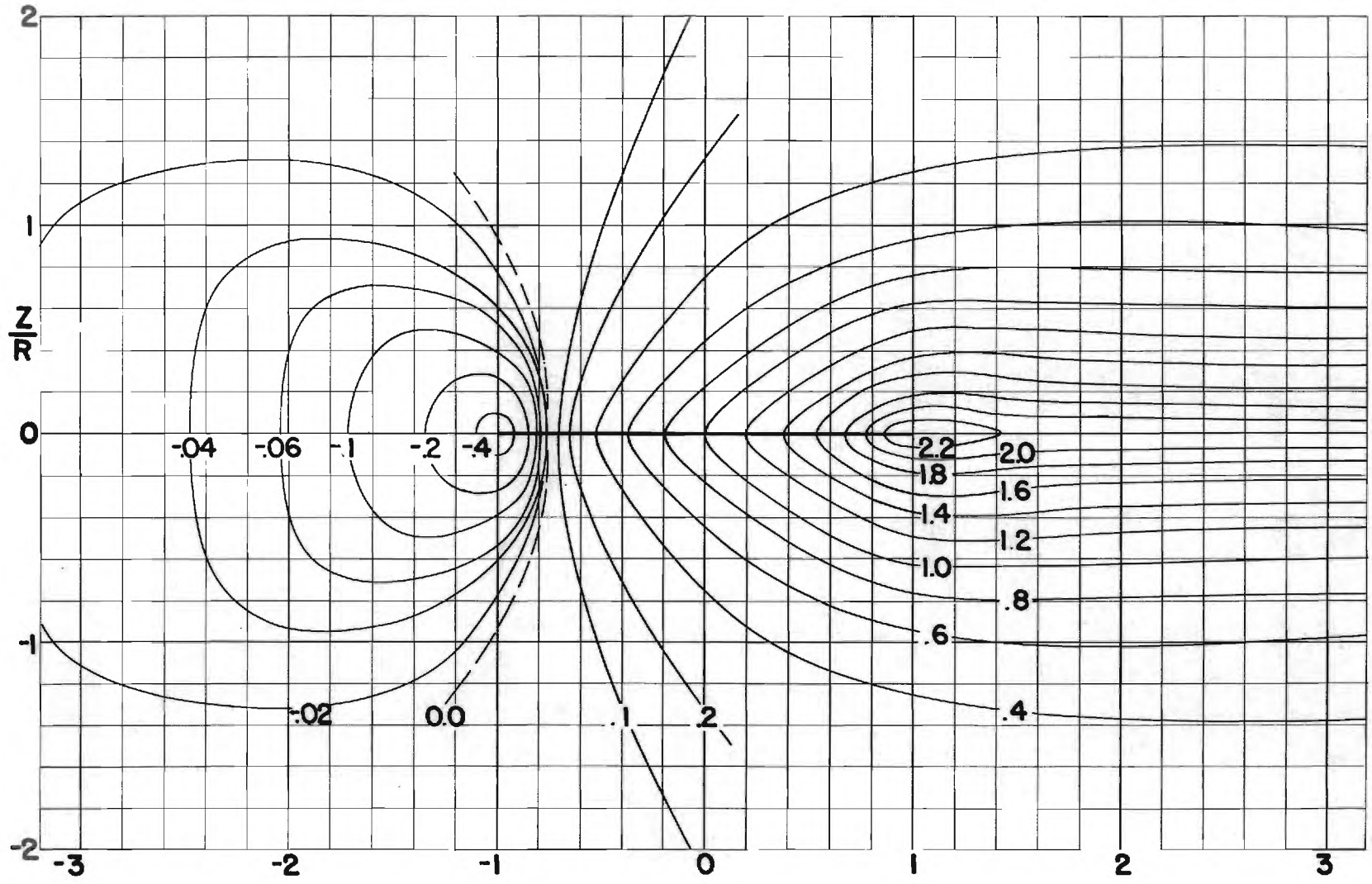

Figure 10. ISO-Induced Velocity Lines for X = 90.0° = TAN^{-1} ∞.

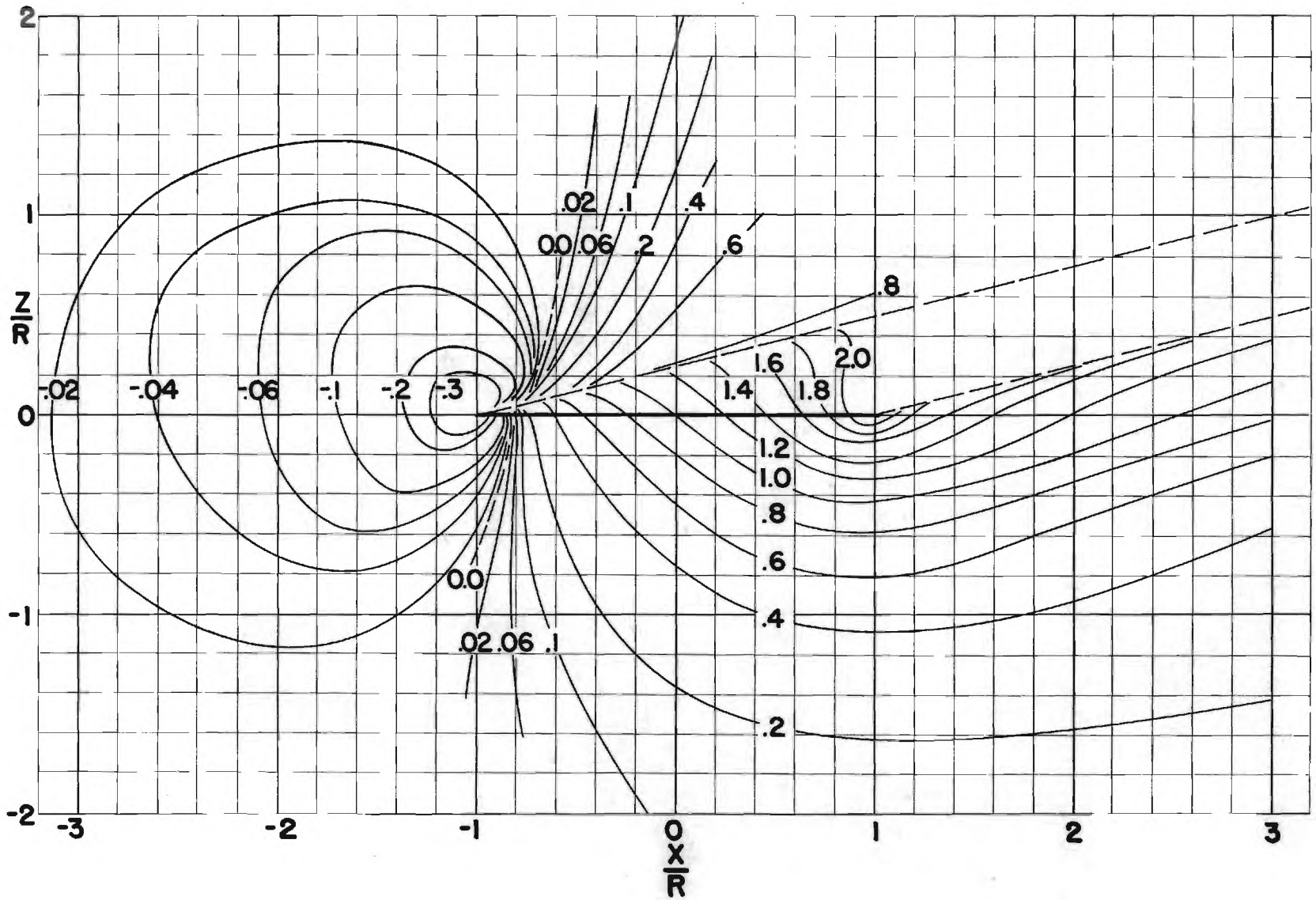

Figure 11. ISO-Induced Velocity Lines for X = 104.0° = TAN^{-1} -4.

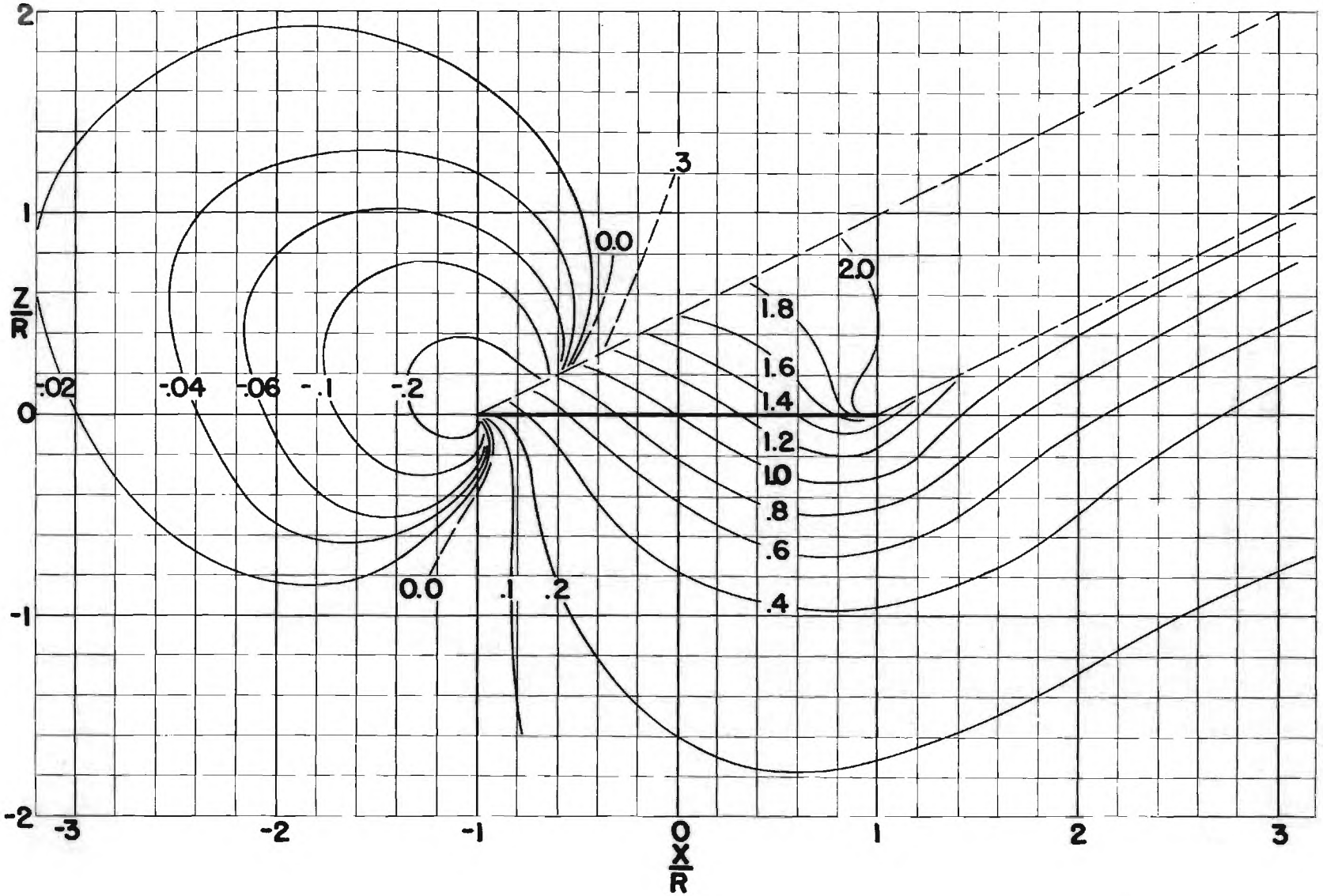

Figure 12. ISO-Induced Velocity Lines for X = 116.6° = TAN^{-1} -2.

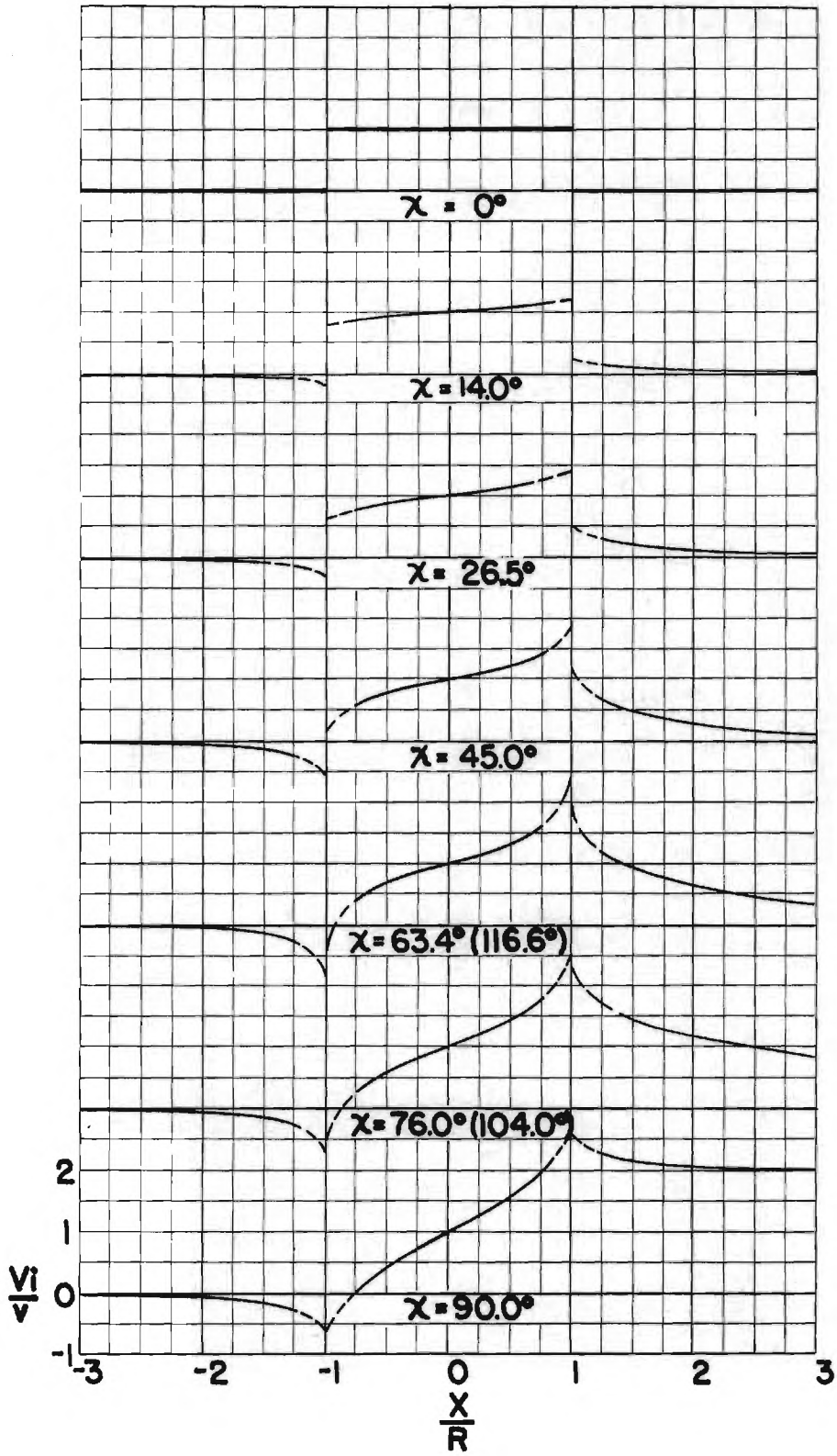

Figure 13. Induced Velocity Distributions Along the Longitudinal Axis.

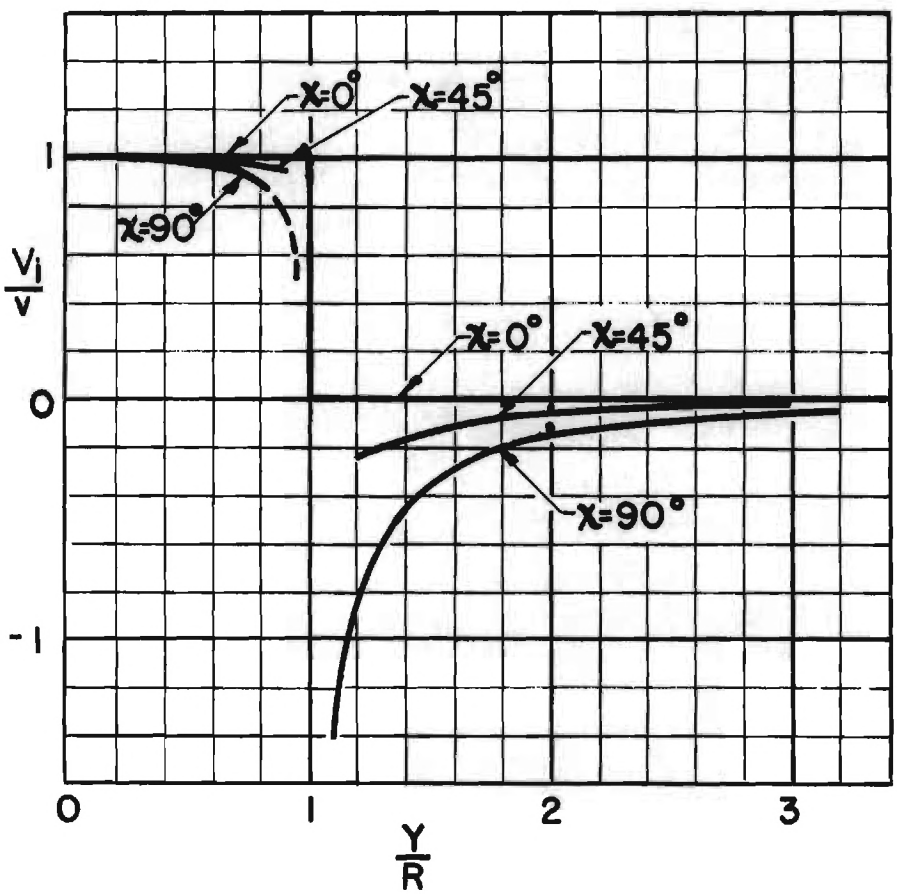

Figure 14. Induced Velocity Distributions Along the Lateral Axis.